available at www.sciencedirect.com

SCIENCE DIRECT®

journal homepage: www.elsevier.com/locate/steroids

Isolation and identification of 2α,25-dihydroxyvitamin D_3, a new metabolite from *Pseudonocardia autotrophica* 100U-19 cells incubated with Vitamin D_3

Koji Takeda[a,*], *Kaichiro Kominato*[a], *Atsuko Sugita*[b], *Yukiko Iwasaki*[c], *Mika Shimazaki*[c], *Masato Shimizu*[c,**]

[a] *Bioresource Laboratories, Mercian Corporation, 1808 Nakaizumi, Iwata, Shizuoka 438-0078, Japan*
[b] *Pharmaceutical Research Department I, Chugai Pharmaceutical Co., Ltd., 1-135 Komakado, Gotenba, Shizuoka 412-8513, Japan*
[c] *School of Biomedical Science, Tokyo Medical and Dental University, 2-3-10 Kanda Surugadai, Chiyoda-ku, Tokyo 101-0062, Japan*

ARTICLE INFO

Article history:
Received 8 February 2006
Received in revised form 1 May 2006
Accepted 3 May 2006
Published on line 19 June 2006

Keywords:
2α,25-Dihydroxyvitamin D_3
Microbial hydroxylation
Pseudonocardia autotrophica
Vitamin D receptor
Vitamin D-binding protein

ABSTRACT

Pseudonocardia autotrophica converted Vitamin D_3 to 25-hydroxyvitamin D_3 and 1α,25-dihydroxyvitamin D_3. The hydroxylation of Vitamin D_3 with *P. autotrophica* was enhanced by the addition of cyclodextrin. In this microbial hydroxylation, a new Vitamin D_3 metabolite was observed in the reaction mixture of *P. autotrophica* and Vitamin D_3, and was isolated in a pure form by several steps of chromatography. The structure of the new metabolite was determined to be 2α,25-dihydroxyvitamin D_3 by UV, NMR and mass spectroscopic analyses. Biological evaluation of the new metabolite was conducted by means of several experiments.
© 2006 Elsevier Inc. All rights reserved.

1. Introduction

Vitamin D_3 (VD_3) exerts its physiological activity by being converted to 25-hydroxyvitamin D_3 (25-OHD_3) in the mammalian liver, and then, in turn, to 1α,25-dihydroxyvitamin D_3 (1α,25-$(OH)_2D_3$) in the kidney [1]. 1α,25-$(OH)_2D_3$ has been clinically used for chronic renal failure, hypoparathyroidism, osteoporosis, and psoriasis [2]. Vitamin D_3 derivatives, the most of which were modified at the A-ring or the side chain of VD_3, have been developed to separate cell differentiation activity from Ca regulation activity [2,3]. Almost all of the VD_3 derivatives have been chemically synthesized by complicated procedures requiring many steps [4]. Some microorganisms, above all, *P. autotrophica* (formerly, *Amycolata autotrophica*), are known to convert VD_3 to 25-OHD_3 and 1α,25-$(OH)_2D_3$ by the cytochrome P450 enzymes [5]. The microbial reaction has an advantage in regio- and stereoselectivity over chemical synthesis, thus making it possible to reduce the number of steps of synthesis. In a microbial hydroxylation of VD_3, partially methylated β-cyclodextrin (PMCD) and γ-cyclodextrin (γ-CD) were very effective in increasing the conversion yield of VD_3 to 25-OHD_3, and 1α,25-$(OH)_2D_3$ [6]. In the presence of cyclodextrin, *P. autotrophica* yielded additional VD_3 metabolites. Because of the obscurity of the metabolism of VD_3 in the presence of *P. autotrophica*, these metabolites may be new discoveries. In this study, we report the isolation, identification, and biological activities of a newly discovered Vitamin D metabolite.

* *Corresponding author*. Tel.: +81 538 36 3188; fax: +81 538 39 2371.
** *Corresponding author*. Tel.: +81 03 5280 8117; fax: +81 03 5280 8005.
E-mail address: takeda-k@mercian.co.jp (K. Takeda).
0039-128X/$ – see front matter © 2006 Elsevier Inc. All rights reserved.
doi:10.1016/j.steroids.2006.05.004

2. Experimental

2.1. Reagents

VD_3 was purchased from Kanto Chemicals Corp. (Tokyo, Japan). PMCD, γ-CD and crystalline 1α,25-$(OH)_2D_3$ are products of Mercian Corp. (Tokyo, Japan). Amberlite XAD-7 was purchased from Organo Corp. (Tokyo, Japan). 1α,25-Dihydroxy[26,27-methyl-^{3}H]cholecalciferol (specific activity 6.62 TBq/mmol) and 25-hydroxy[26,27-methyl-^{3}H]cholecalciferol (specific activity, 6.66 TBq/mmol) were purchased from Amersham (Buckinghamshire, U.K.). Vitamin D receptor (VDR) binding assays were carried out using a chicken intestinal VDR kit (Yamasa Shoyu Co., Ltd., Chiba, Japan). Clear-sol I scintillation fluid was obtained from Nacalai Tesque (Kyoto, Japan). All of the organic solvents were of high-performance liquid chromatography (HPLC) grade. The concentrations of standard solutions of Vitamin D compounds were determined by ultraviolet (UV) spectroscopy using the molar absorptivity (ε = 18,200) at 265 nm in 95% ethanol (EtOH).

2.2. General procedure

The nuclear magnetic resonance (NMR) spectra were recorded on a Bruker ARX-400 MHz spectrometer, operating at 400 MHz for ^{1}H and 101 MHz for ^{13}C. Chemical shifts are reported in parts per million (ppm, δ) downfield from tetramethylsilane as an internal standard (δ 0 ppm) for ^{1}H and ^{13}C NMR. Low- and high-resolution mass spectra (LR- and HL-MS) were obtained with electronic ionization (EI) on a JEOL TMS-AX-505HA spectrometer. All spectra were run at 70 eV for EI and *m/z* values are given with relative intensities in parentheses. UV spectra were obtained on a Beckmann DU-7000 spectrophotometer.

HPLC was performed with a JASCO HPLC system equipped with a Model PU-980 intelligent pump and a Model MD-910 photodiode array detector. Purification of the VD_3 metabolites was achieved with: (1) a centrifugal partition chromatograph (CPC; SANKI Engineering, Ltd.) using the upper phase of solvent mixture (ethyl acetate (AcOEt)/*n*-hexane/methanol (MeOH)/water (6:4:5:5)) as the stationary phase, and the lower phase of same mixture as the mobile phase in the ascending mode at a flow rate of 20 mL/min; (2) a normal-phase LiChrosorb Si 60 (250 mm × 10 mm, particle size 7 μm) (Cica-Merck, Tokyo, Japan) eluted with 15% 2-propanol in hexane at a flow rate of 6 mL/min.

2.3. Bioconversion of VD_3

The strain 100U-19 was derived from the treatment of *P. autotrophica* FERM BP-1573 with *N*-methyl-*N*′-nitro-*N*-nitrosoguanidin (Fig. 1). The cultivation and conversion of VD_3 with *P. autotrophica* were carried out in a 2 KL-tank fermentor using an already reported method [6], except that 0.05% (w/v) of PMCD and 0.2% (w/v) of γ-CD were supplied. After 48 h cultivation, 200 g of VD_3 in 1.0 L of EtOH was added to

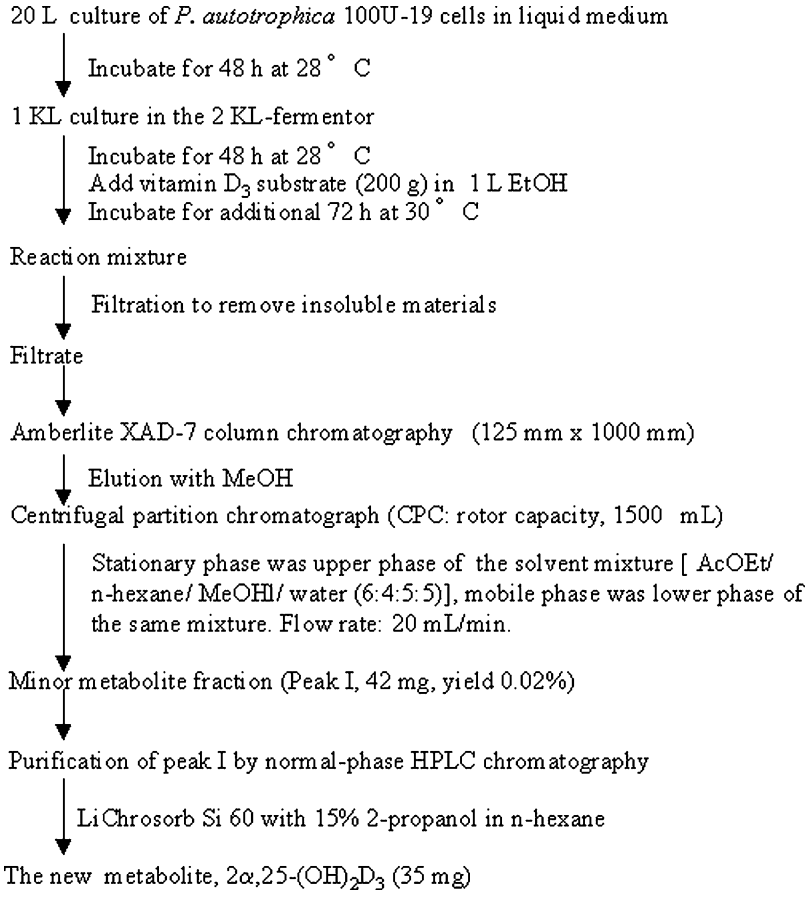

Fig. 1 – Microbial transformation of Vitamin D_3

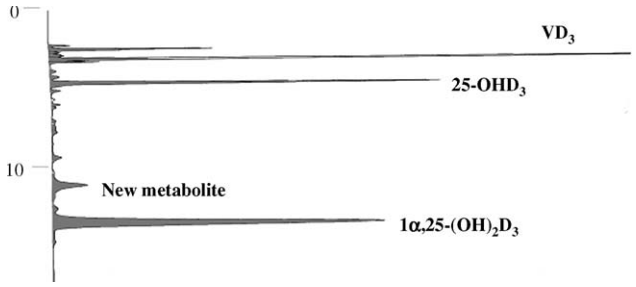

Fig. 2 – HPLC profile of the Vitamin D metabolites produced from Vitamin D_3 by incubation with *P. autotrophica*. Normal-phase HPLC (Zorbax SIL, 4.6 mm × 250 mm, 14% 2-propanol in *n*-hexane, 1.5 mL/min) chromatogram of the lipid extracts after extraction of the incubation mixture by modified Bligh and Dyer method.

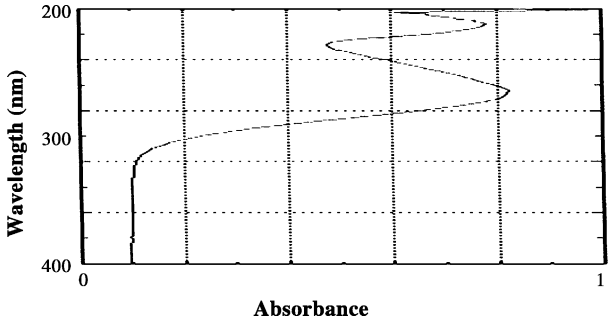

Fig. 4 – UV absorption spectrum of the new metabolite recorded in 95% ethanol solution.

the culture broth of *P. autotrophica*, the cultivation was continued for a further 72 h at 30 °C. To investigate the conversion yield by the microbial hydroxylation of substrate at this stage, a small portion of the reaction mixture was extracted with MeOH–dichloromethane by the modified Bligh and Dyer method [7], and then the lipid residue was analyzed by HPLC using Zolbax SIL (4.6 mm × 250 mm particle size 5 μm) (Du Pont, Wilmington, USA) eluted with 14% 2-propanol in *n*-hexane at a flow rate of 1.5 mL/min (Fig. 2).

2.4. *Isolation and purification of the new metabolite of Vitamin D_3*

The isolation procedure is summarized in Fig. 1. Although most VD_3 metabolites are water-insoluble, VD_3 metabolites under this condition were present in water-soluble form as a result of the effect of cyclodextrin. Consequently, the isolation was started by the filtration of the reaction mixture to remove insoluble material. An Amberlite XAD-7 column was conditioned with water, and the clear filtrate (~1 KL) was loaded onto it. The column was eluted with water (200 L), 30% (v/v) MeOH in water (300 L), and 100% MeOH (150 L), while analysis was performed on a UV detector with detection by UV absorption at 265 nm. The MeOH fraction (~50 L) containing the hydroxylated Vitamin D metabolites was collected and diluted with water (10 L). The whole mixture was concentrated in vacuo to a small volume, at which time the precipitate appeared. The solid was filtered through the filter paper and vacuum-dried. The resulting dried material was applied to the CPC equipped with cells (rotor capacity, 1.5 L). The CPC instrument was filled with the upper phase obtained from the solvent mixture (AcOEt/*n*-hexane/MeOH/water (6:4:5:5)) as the stationary phase, and samples (5.0 g) dissolved in AcOEt (5.0 mL) were chromatographed on the CPC eluted with the lower phase from the same solvent mixture described above at a flow rate of 20 mL/min (Fig. 3A). The fractions containing the peak I (and eluted between 690 and 720 mL) were pooled, and evaporated in vacuo to give the new metabolite (42 mg) in an almost pure form. This metabolite was further purified by normal-phase HPLC (LiChrosorb Si 60; 10 mm × 250 mm; 15% 2-propanol in *n*-hexane; 6 mL/min) to afford the pure peak I (35 mg) (Fig. 3B), which was subjected to spectral analysis. The UV, mass, and ^{1}H NMR spectra are shown in Figs. 4–6, respectively.

2.4.1. *Spectral data of the new metabolite (peak I)*

UV λ_{max} (95% EtOH): 265 nm. MS *m/z* (%): 416 (M^+, 49); 398 (21); 383 (21); 380 (10); 365 (14); 362 (5); 287 (17); 269 (10); 251 (9); 192 (15); 174 (24); 152 (100); 134 (49). HR-EI-MS *m/z*: 416.3289 (calcd

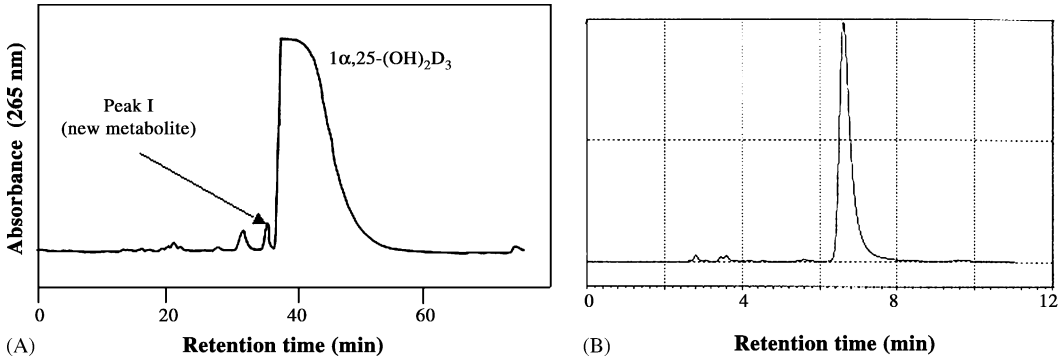

Fig. 3 – Elution profile of the CPC after separation by Amberlite XAD-7 and HPLC chromatogram after purification by the CPC. (A) CPC [rotor capacity, 1500 mL; stationary phase, upper phase of the solvent mixture (AcOEt/*n*-hexane/MeOH/water = 6/4/5/5); mobile phase, lower phase of the same solvent; 20 mL/min] elution pattern after the Amberlite XAD-7 chromatography. (B) Normal-phase HPLC (LiChrosorb Si 60; 10 mm × 250 mm; 15% 2-propanol in *n*-hexane; 6 mL/min) chromatogram of the isolated peak I.

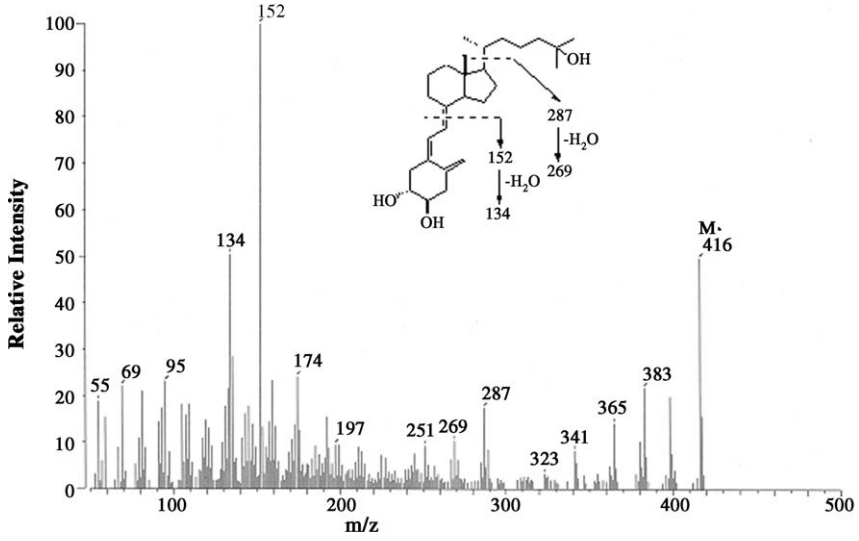

Fig. 5 – Mass spectrum of the new metabolite.

for $C_{27}H_{44}O_5$: 416.3290). ^{1}H NMR ($CDCl_3$) δ: 0.54 (3 H, s, 18-H); 0.93 (3 H, d, J = 6.4 Hz, 21-H); 1.22 (6 H, s, 26, 27-H); 2.13–2.28 (3 H, m); 2.62 (2 H, m, 1, 4-H); 2.82 (1 H, m, 9-H); 3.59 (2 H, m, 2, 3-H); 4.91 (1 H, 19-H); 5.12 (1 H, 19-H); 5.99 (1 H, d, J = 11.3 Hz, 7-H); 6.27 (1 H, d, J = 11.3 Hz, 6-H). ^{13}C NMR ($CDCl_3$) δ: 12.3; 19.0; 21.0; 22.3; 23.7; 27.9; 29.2; 29.4; 29.5; 36.3; 36.6; 40.7; 41.2; 42.2; 44.6; 46.1; 56.5; 56.7; 71.4; 74.8; 75.1; 115.2; 117.6; 122.9; 134.2; 141.9; 143.3

2.5. *Vitamin D receptor binding assay*

Each compound whose binding affinity was assayed was serially diluted with EtOH. Then, 5 μL of diluted compound was mixed with 5 μL of 1α,25-dihydroxy[26,27-methyl-^{3}H]cholecalciferol (radioactivity, 172.7 Bq) in EtOH; 500 μL of chicken intestinal VDR diluted with phosphate buffer (0.3 mol/L KCl, 5 mmol/L DTT, 0.03 mol/L K_2HPO_4, 0.01 mol/L KH_2PO_4) was added; and the total mixture was well mixed (n = 2). It was allowed to stand for 3 h in a refrigerator set at 4 °C; then 125 μL of dextran-coated charcoal suspension (Yamasa Shoyu Co., Ltd.) was added, and the mixture was left to stand in ice water for 30 min. Next, bound-free (B-F) separation (separation of compound bound to VDR [B] from compound unbound to VDR [F]) was carried out by centrifugation (05PR-22, Hitachi, Ltd.) at 3000 rpm for 15 min at 4 °C. Then, a 0.5 mL aliquot of the supernatant was thoroughly mixed with 5.0 mL of Clear-sol I in each vial, and radioactivity was measured with a liquid scintillation counter (Tri-Carb 2700TR, Perkin Elmer, Inc.).

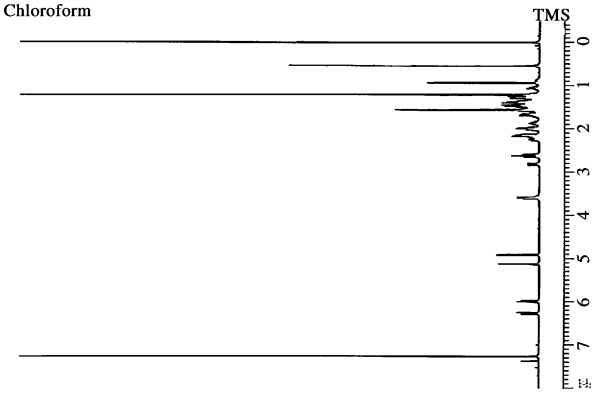

Fig. 6 – ^{1}H NMR spectrum of the new metabolite taken in chloroform-d_1. TMS: tetramethylsilane.

2.6. *Vitamin D-binding protein (DBP) binding assay*

Each compound whose binding affinity was assayed was serially diluted with EtOH (diluted at time of use). Then 50 μL of diluted compound was mixed with 50 μL of 25-hydroxy[26,27-methyl-^{3}H]cholecalciferol (radioactivity, 231.25 Bq) in EtOH solution, and 1 mL of rat serum diluted 70,000-fold with barbital buffer (3.5 mmol/L CH_3COONa, 3.5 mmol/L barbital sodium, 0.13 mol/L NaCl, pH 8.6) containing 0.1% ovalbumin was added (n = 2). The mixture was allowed to stand for 1 h in a refrigerator set at 4 °C; 0.5 mL of dextran-charcoal (0.025% dextran and 0.25% charcoal in barbital buffer) was added; further mixing was performed; and the mixture was allowed to stand in ice water for 10 min. Next, B-F separation (of compound bound and not bound to serum DBP) was carried out by centrifugation (05PR-22; Hitachi, Ltd.) at 3000 rpm for 15 min at 4 °C. Finally, 5.0 mL of Clear-sol I was added to 1.0 mL of the supernatant; thorough mixing was performed; and radioactivity was measured with a liquid scintillation counter (Tri-Carb 2700TR).

2.7. *Vitamin D responsive element (VDRE) reporter gene assay*

COS-1 cells were grown in DMEM media supplemented with 10% charcoal dextran stripped fetal bovine serum (FBS), and transient transfection was done using Superfect transfection reagent (Qiagen), following the manufacturer's recommendations.

All procedures were done according to the Dual-Luciferase Reporter Assay System (Promega). COS-1 cells were seeded in flat-bottomed 96-well plates (2×10^3 cells/well). After they had

adhered, cells were temporarily transfected with pGL3 Basic containing three copies of the Vitamin D response element (3 × VDRE), and the pRL SV40 internal control plasmid. After 6 h, various concentrations of the new metabolite and 1α,25-$(OH)_2D_3$ were added, and the cells were incubated for 40 h at 37 °C. Cells were lysed using a passive lysis buffer and analyzed on a microplate luminometer (ARVO, Wallac).

2.8. Human promyeloid leukemia (HL-60) differentiation-inducing assay

HL-60 cells were grown in RPMI-1640 media supplemented with 10% heat-inactivated FBS and 20 μg/mL of gentamicin. Induction of differentiation was estimated from the ability of the cell to generate superoxide anion. Vitamin D-induced cells were obtained by seeding HL-60 cells at 1×10^5 mL^{-1} in growth media and culturing them for 4 days in the presence of various concentrations of Vitamin D_3 analogues. The cells were washed free of the compounds and suspended in a 1.5 mL reaction mixture containing 80 μM of ferricytochrome C (Sigma) and 500 ng/mL phorbol myristate acetate (Sigma) in a 0.1% gelatin Hanks' balanced salt solution without phenol red. The mixture was incubated at 37 °C for 60 min and centrifuged for 10 min at 400 × *g* at 4 °C. The optical density of the supernatant was determined with a Hitachi U-3200 dual-wavelength (540–550 nm) spectrophotometer. The amount of superoxide anion generated was calculated with a molar extinction coefficient of 19.1×10^3 cm^{-1}. Deoxidization cytochrome C concentration (nmol/L) = the amount of superoxide anion generated = $[(OD550 - OD540)/(19.1 \times 10^3) \times 1.5]/10^3 \times 10^9$.

2.9. Keratinocyte growth inhibition assay

Normal human keratinocytes (Sanko Junyaku Co., Ltd.) were grown in serum-free media (KGM-2, Sanko Junyaku Co., Ltd.). The cells were plated in 96-well plates at 2×10^3 cells/175 μL/well. The test substance and the control substance were diluted with KGM-2 media and then 25 μL of each diluted solution was added to separate wells (test substance: $n = 6$, control substance: $n = 12$). After addition of the drugs, the cells were cultured for 3 days. [Methyl-^{3}H]thymidine was diluted with KGM-2 media. Then, 25 μL of this diluted solution (7.4 kBq) was added to each well, and the cells were cultured overnight. The cells were then detached by 0.05% trypsin–EDTA in PBS (−). Next, the cells were adsorbed onto a filter (Printed Filtermat A, Perkin Elmer Japan Co., Ltd.), with a cell harvester (Harvester 96 Mach III M, Tomtec Inc.), and the filter was dried in a microwave oven. The filter was then embedded in a scintillator (MeltiLex A, Perkin Elmer Japan Co., Ltd.), and the radioactivity taken up by the cells was measured with a liquid scintillation counter (MicroBeta 1450, Wallac Oy).

3. Results and discussion

3.1. Bioconversion of VD_3

VD_3 was mainly converted to 25-OHD_3 and 1α,25-$(OH)_2D_3$ after reacting for 72 h. The concentrations of 25-OHD_3 and 1α,25-$(OH)_2D_3$ were 7.8 and 32 mg/L, respectively. The new metabolite was detected by HPLC (Fig. 2), and its amount represented about 8% of that of 1α,25-$(OH)_2D_3$, based on the HPLC peak area.

3.2. Identification and structural elucidation of the new Vitamin D_3 metabolite

A flow sheet of the procedures used in the isolation of the metabolite is shown in Fig. 1. After removal of the substrate VD_3 and hydrophilic substance by Amberlite XAD-7 column, the fraction containing the more polar Vitamin D metabolites was purified on a CPC equipped with the upper phase of the solvent mixture (AcOEt/*n*-hexane/MeOH/water (6:4:5:5)) as the stationary phase, the lower phase of same mixture as the mobile phase. The peak containing a new metabolite was eluted just before the elution of 1α,25-$(OH)_2D_3$, which was observed as a major peak in this condition (Fig. 3A). Peak I was collected and was rechromatographed on a LiChrosorb Si 60 column with 15% (v/v) 2-propanol in hexane (Fig. 3B). By means of this procedure, the new metabolite of Vitamin D_3 has been isolated in pure form. The structure of this new metabolite has been unequivocally identified as 2α,25-$(OH)_2D_3$ by means of UV absorption, mass, and NMR spectrometry.

The UV spectrum of the new metabolite isolated in its pure form is presented in Fig. 4. The spectrum displays a λ_{max} at 265 nm and a λ_{min} 228 nm, exhibiting the presence of the conjugated triene chromophore typical of VD_3.

The low-resolution mass spectrum of the new metabolite is presented in Fig. 5. The mass spectrum exhibited an apparent molecular ion (M^+) at *m/z* 416. High-resolution mass spectrometry of the metabolite revealed a molecular weight of 416.3289, and the elemental composition was determined to be $C_{27}H_{44}O_3$ (calcd for $C_{27}H_{44}O_3$, 416.3290). The molecular formula indicates the incorporation of two additional oxygen atoms into the starting substrate VD_3 (*m/z* 284, M^+). Fragment ions resulting from the cleavage at the C(7)–C(8) double bond and the elimination of the side chain are highly diagnostic for the structural assignments of the Vitamin D compound [8,9]. Characteristic ions at *m/z* 152 and 134 arising from the dissociation of the C(7)–C(8) bond and from the subsequent elimination of water, respectively, confirm the presence of two hydroxyl groups on the A-ring. It is interesting to note that in contrast with 1α,25-$(OH)_2D_3$ (*m/z* 134 as a base peak), the ion at *m/z* 152 was observed as a base peak in the new metabolite. This ion shows that the 3β-hydroxyl group from the substrate is present in the A-ring and the additional hydroxyl group is either at the C(2) or the C(4) position. Fragment ions at *m/z* 287 resulting from the cleavage at the C(17)–C(20) bond suggests the presence of the other oxygen atom on the side chain. The location of the hydroxyl group on the side chain cannot be deduced from the mass spectral data.

Fig. 6 illustrates the ^{1}H NMR spectrum of the new metabolite. The spectrum afforded definite evidence for the structure of the metabolite. It showed the typical resonance for the olefinic protons of the Vitamin D 5,6-*cis* triene chromophore: two AB-type doublets at δ 6.27 and 5.99 ppm for the C(6) and C(7) protons, and two multiplets assigned to the C(19) protons at δ 4.91 and 5.12 ppm, whose chemical shifts are almost identical with those observed in the starting VD_3 [10,11]. The

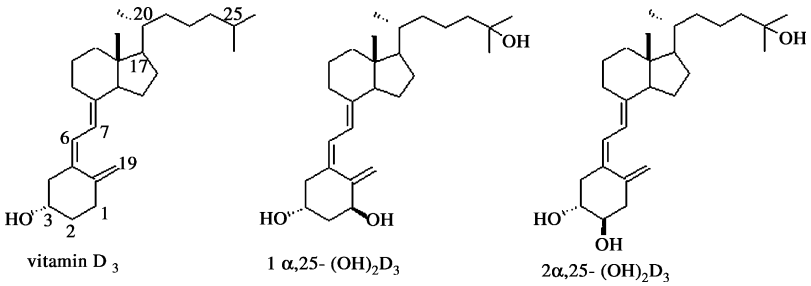

Fig. 7 – Structure of Vitamin D_3, 1α,25-$(OH)_2D_3$ and 2α,25-$(OH)_2D_3$.

six-proton singlet at δ 1.22 ppm can be assigned to the 26- and 27-methyl groups. This signal is shifted downfield when compared with the spectrum of the starting VD_3 (δ 0.86 ppm). This, together with the mass spectrum data mentioned above, strongly suggests the presence of the hydroxyl function at the position of C(25). The multiplet signal centered at δ 3.59 was ascribed to the two methine protons attached to the hydroxyl groups in the A-ring. This signal appears at higher field than the general methine absorption of the starting VD_3 and its metabolites, 1α,25-$(OH)_2D_3$ at C(3) and/or C(1). In the COSY spectrum of the new metabolite, the two-proton multiplet signals at δ 3.59 ppm strongly interact with four protons from the A-ring resonating at δ 2.1–2.7 ppm. From the chemical shift values, these protons can be assigned to the methylene positions at C(1) and C(4) positions. This strongly suggested that an additional hydroxyl group in the A-ring is present at the C(2) position. The position and the configuration of the newly introduced hydroxyl group in the A-ring were determined by comparing with the ^{1}H NMR spectral data of both 2α-hydroxyvitamin D_3 (2α-OHD_3) and 2β-hydroxyvitamin D_3 (2β-OHD_3) reported by Kaneko et al. [12,13]. The ^{1}H NMR spectrum of 2α-OHD_3 showed the resonance of the C(2)- and C(3)-protons with a chemical shift (δ 3.55 ppm) almost identical with that observed in the new metabolite (δ 3.55 ppm), whereas two separated multiplet C(2)- and C(3)-protons (δ 4.07 and 4.33 ppm) were observed in the spectrum of 2β-OHD_3. Therefore, the structure of the new metabolite was established to be 2α,25-$(OH)_2D_3$ [14] (Fig. 7). Both signals at the C(2)- and C(3)-protons in 2α-OHD_3 are shifted by 0.5–0.8 ppm upfield with respect to those of the corresponding 2β-isomer. The equatorial protons are usually observed at a lower field than the axial protons [15]. Thus, on the basis of the NMR characteristics, both C(2) and C(3) protons of the isolated metabolite is axial, appearing as multiplet signals at δ 3.59 ppm.

The A-ring conformation of 1α,25-$(OH)_2D_3$ involves mainly the two chair forms in solution as shown in Fig. 8. These conformers exist in a dynamic equilibrium, abbreviated as α-conformer with an axial 1α-hydroxyl group and an equatorial 3β-hydroxyl group, and β-conformer with both an equatorial 1α- and an axial 3β-hydroxyl group (Fig. 8) [16]. Based on the analysis of ^{1}H NMR spectrum, the A-ring of the new metabolite assumes to be the α-conformation in which both 2α- and 3β-hydroxyl groups are equatorially oriented, although due to signals overlapping, the coupling constant between H-2 and H-3 was difficult to estimate.

3.3. *Biological evaluations of the new metabolite*

3.3.1. *VDR binding affinity*

We evaluated the affinity of the new metabolite, 2α,25-$(OH)_2D_3$ to bind to VDR from chicken intestine. The affinity for VDR was determined by a competitive binding assay between radioactive 1α,25-$(OH)_2D_3$ and 2α,25-$(OH)_2D_3$. 2α,25-$(OH)_2D_3$ was about 100 times less active than the natural ligand, 1α,25-$(OH)_2D_3$. In the recent crystal structure of VDR ligand binding domain (LBD) in complex with 1α,25-$(OH)_2D_3$ and its derivatives, the natural ligand harbored in the ligand binding pocket (LBP) adopts the β-conformation at the A-ring [17–20]. VDR is able to bind ligands with the A-ring in the β-conformation. The three hydroxyl groups of 1α,25-$(OH)_2D_3$ made the hydrogen bonds, 1α-OH with Ser237 and Arg274, 3β-OH with Tyr143 and Ser278, and 25-OH with His305 and His397. The Arg274 residue is essential to anchor the 1α-OH group of the natural hormone with the hydrogen bond. 2α,25-OHD_3 causes loss of a critical hydrogen bond to the Arg274, which may result in ca. 100-fold decrease in binding to the VDR. Furthermore, in the solution state, the isolated metabolite prefers the α-conformation as shown in ^{1}H NMR spectrum. The low-energy A-ring α-conformation of 2α,25-$(OH)_2D_3$ must change the high-energy β-conformation to accommodate in the VDR LBP. In this conformation, both 2α- and 3β-hydroxyl groups occupy the energetically unfavorable axial positions. Within the VDR LBP, on

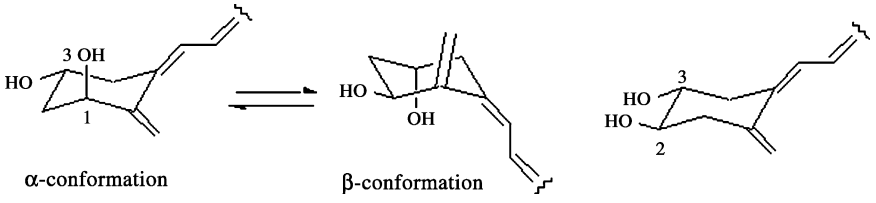

Fig. 8 – A-ring conformations under dynamic equilibrium of 1α,25-$(OH)_2D_3$ and the α-conformer of 2α,25-$(OH)_2D_3$. The A-ring of 1α,25-$(OH)_2D_3$ exists as an approximate equimolar mixture of two coformation, whereas that of 2α,25-$(OH)_2D_3$ exists predominantly in α-conformation.

the β-face a narrow space is open for the hydrophobic interaction with adjacent LBP amino acid residues, Leu233, Phe150 and the phenyl ring of Tyr236, while the hydrophilic Arg274, Ser275 and Tyr143 are present on the α-face of the A-ring [21]. The hydrophilic 2α-hydroxyl group points towards the hydrophobic environment. The metabolite can make the unfavorable interactions within the LBP, explaining the decreased binding affinity for VDR.

3.3.2. *DBP binding assay*

The binding affinity of the new metabolite for DBP was 114 times more active than 1α,25-$(OH)_2D_3$, and about two-fold less potent than 25-OHD_3, which is the natural Vitamin D_3 metabolite with the highest affinity for the DBP. The three-dimensional structure of DBP in complex with 25-OHD_3 was determined recently [22]. The Vitamin D-binding site is located in the N-terminal region and lined by hydrophobic residues. The α-side of 25-OHD_3 is docked in DBP binding cleft and part of the β-side of the C/D-ring has no interaction with DBP (for example part of the surface molecule contacts with the surrounding solvent). In the DBP cleft, the A-ring of 25-OHD_3 adopts the α-chair conformation. The 25-hydroxyl group of 25-OHD_3 is hydrogen-bonded to Tyr32 and the 3β-hydroxyl group contacts Ser76 and Met107. From the ^{1}H NMR analysis, the A-ring of the new metabolite adopts the same α-conformation as 25-OHD_3. The high affinity of the metabolite for DBP can be explained that the metabolite binds to DBP with energetically stable α-conformation, and the amino acid residues Tyr32, Ser76 and Met107 are expected to stabilize the molecule via the hydrogen bonds with the hydroxyl groups at C(3) and C(25). Docking studies of 2α,25-$(OH)_2D_3$ with DBP using the docking software Flex X (Tripos, St. Louis) show that the backbone carbonyl of Met107 contacts the 2α-hydroxy group in 2α,25-$(OH)_2D_3$, whereas Ser76, Ser79 and Met107 form hydrogen bond with the 3β-hydroxy moiety (Fig. 9). Thus, the A-ring is stabilized in the DBP binding cleft by hydrophilic interactions. 1α,25-$(OH)_2D_3$ has an extremely lower affinity for DBP than 25-OHD_3. 1α,25-$(OH)_2D_3$ binds to DBP with the A-ring α-conformation. Interaction of an axial 1α-hydroxyl group with nearby Met107 in helix 6 may cause sterical hindrance. This might be explained the decreased DBP binding affinity for 1α,25-$(OH)_2D_3$.

Among the synthetic Vitamin D analogs, the highest affinity for DBP is observed for 22-(*p*-hydroxyphenyl)-23,24,25,26,27-pentanor-Vitamin D_3 [22]. The 2β-substituted 1α,25-$(OH)_2D_3$ analogs have a higher affinity for DBP than the corresponding the 2α-isomers, indicating that the orientation of the C(2) position may be correlated with the increased abilities to bind the DBP [23]. Major function of DBP includes binding of Vitamin D_3 and its metabolites for their biological actions. Expression profiles of biological activities of synthetic Vitamin D analogs have been often linked to their DBP binding affinity [3]. Detailed structure–activity studies on DBP–Vitamin D analogs will be helpful for developing the new analogs having a more selective activity.

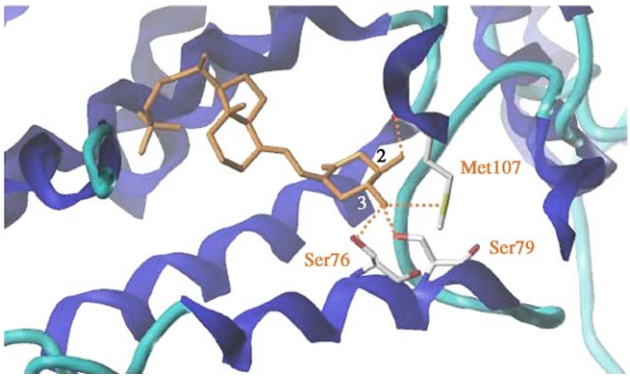

Fig. 9 – Docking model of 2α,25-$(OH)_2D_3$ docked into DBP and its interacting amino acid residues.

3.3.3. *Other biological activities*

The potencies of 2α,25-$(OH)_2D_3$ were examined by determining its luciferase-activating activity, cell-differentiating activity, and antiproliferative effects. Results obtained in vitro studies are given in Table 1. 2α,25-$(OH)_2D_3$ was less active in induction of gene transactivation, stimulating cell differentiation and inhibiting cell proliferation as compared to the native hormone, 1α,25-$(OH)_2D_3$.

VDR-mediated transcriptional activity of 2α,25-$(OH)_2D_3$ was tested in COS-1 cells. 2α,25-$(OH)_2D_3$ was found to be about 180 times less potent than 1α,25-$(OH)_2D_3$ (Fig. 10A). The EC50 values for transcriptional activity ($n=3$) are 1α,25-$(OH)_2D_3$ 2.93×10^{-10} M and 2α,25-$(OH)_2D_3$ 5.25×10^{-8} M, respectively. The extremely low transcriptional potency of 2α,25-$(OH)_2D_3$ may be explained as follows: the metabolite lacks 1α-hydroxyl

Table 1 – Relative potency of 2α,25-$(OH)_2D_3$ with respect to 1α,25-$(OH)_2D_3$

	Binding affinity		Trans. activity[c]	Cell differentiation and proliferation	
	VDR[a]	DBP[b]		HL-60[d]	Keratinocytes[e]
1α,25-$(OH)_2D_3$	100	100	100	100	100
2α,25-$(OH)_2D_3$	1.14	11434	0.56	3.28	23

Trans. activity: transcriptional activity. The potencies of 1α,25-$(OH)_2D_3$ are normalized to 100.

[a] The binding affinity for the chicken intestinal VDR.

[b] The binding affinity for the rat serum Vitamin D-binding protein.

[c] Gene-activating activity at Vitamin D response element-luciferase reporter gene in COS-1 cells.

[d] Differentiation inducing effect on HL-60 cells.

[e] Inhibition of proliferation of human keratinocyte cells.

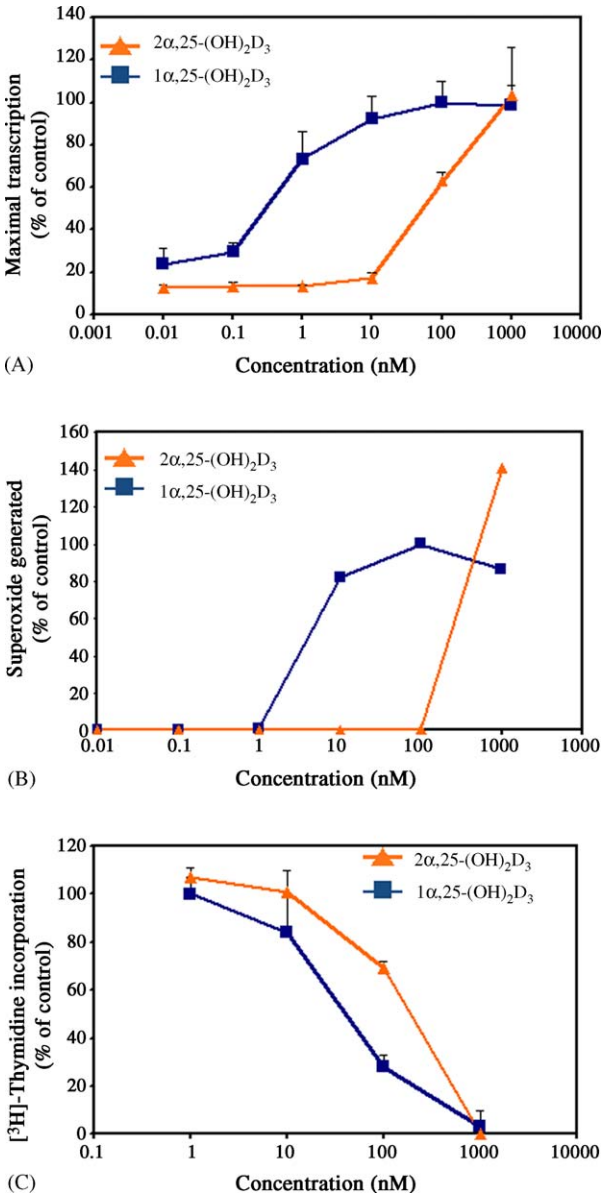

Fig. 10 – Biological activities of 2α,25-$(OH)_2D_3$. (A) Transcriptional potency of 2α,25-$(OH)_2D_3$ on a VDRE-luciferase reporter gene in COS-1 cells. (B) Dose–response effects of 2α,25-$(OH)_2D_3$ on the induction of superoxide production in HL-60 cells. (C) Dose–response effect of 2α,25-$(OH)_2D_3$ on cell proliferation of human keratinocytes.

group that is considered essential for high genomic activity, and a high DBP affinity leads to inactivation because only unbound portions of 2α,25-$(OH)_2D_3$ have biological activity.

The differentiating effects of 2α,25-$(OH)_2D_3$ on HL-60 cells was about 30 times weaker than that of 1α,25-$(OH)_2D_3$ (Fig. 10B). The EC_{50} values from dose–response curve in HL-60 cell differentiation ($n = 1$) are 6.1×10^{-9} M for 1α,25-$(OH)_2D_3$ and 1.9×10^{-7} M for 2α,25-$(OH)_2D_3$, respectively. 2α,25-OHD_3 exhibited the transcriptional activity only at 1 μM, and the graphs in Fig. 10B make the interpretation of clear correlation between transcriptional activity and the activity of HL-60 cell differentiation difficult. For the antiproliferation properties in human keratinocyte, 2α,25-$(OH)_2D_3$ was about four-fold less active, but it did have significant antiproliferation potency, 23% of that of 1α,25-$(OH)_2D_3$ (Fig. 10C). The activity of 2α,25-$(OH)_2D_3$ between VDR-mediated transactivation and inhibition of cell proliferation was not parallel. Luciferase assay and cell proliferation experiments were carried out in different cells. In addition, keratinocyte growth inhibition assay was conducted in FBS-free medium. These may explain the extremely low gene transactivation and the high inhibition of cell proliferation.

In conclusion we have demonstrated the new Vitamin D metabolite, 2α,25-$(OH)_2D_3$ which was produced from the microbial hydroxylation of VD_3 with *P. autotrophica*. Transposition of 1α-OH group into C(2) position did markedly alter the binding properties for the VDR, whereas it caused a DBP affinity up to 114-fold as compared to 1α,25-$(OH)_2D_3$. This new metabolite showed considerable antiproliferation potency. Isolation of noble Vitamin D metabolites from the reaction mixture is now under investigation.

REFERENCES

[1] DeLuca HF, Schnoes HK. Vitamin D. Recent advances. Annu Rev Biochem 1983;52:411–39.
[2] Glorrieu FH, Pike JW, editors. Vitamin D. New York: Academic; 1997.
[3] Bouillon R, Okamura WH, Norman AW. Structure–function relationships in the Vitamin D endocrine system. Endocr Rev 1995;16:200–57.
[4] Zhu G-D, Okamura WH. Synthesis of Vitamin D (calciferol). Chem Rev 1995;95:1877–952.
[5] Sasaki J, Miyazaki A, Saito M, Adachi T, Mizoue K, Hanada K, et al. Transformation of Vitamin D_3 using *Amycolate* sp. Strains. Appl Microbiol Biotechnol 1992;38:152–7.
[6] Takeda K, Asou T, Matsuda A, Kimura K, Okamura K, Okamoto R, et al. Application of cyclodextrin to microbial transformation of Vitamin D_3 to 25-hydroxyvitamin D_3 and 1α,25-dihydroxyvitamin D_3. J Ferment Bioeng 1994;78:380–2.
[7] Lund J, DeLuca HF. Biologically active metabolite of Vitamin D_3 from bone, liver, and blood serum. J Lipid Res 1991;7:739–44.
[8] Blunt JW, DeLuca HF, Schnoes HK. 25-Hydroxycholecalciferol. A biologically active metabolite of Vitamin D_3. Biochemistry 1968;7:3317–22.
[9] Holick MF, Schnoes HK, DeLuca HF, Suda T, Cousins RJ. Isolation and identification of 1,25-dihydroxycholecalciferol. A metabolite of Vitamin D active in intestine. Biochemistry 1971;10:2799–804.
[10] Wing RM, Okamura WH, Rego A, Perio MR, Norman AW. Studies on Vitamin D and its analogs. VII. Solution conformations of Vitamin D_3 and 1α,25-dihydroxyvitamin D_3 by high-resolution proton magnetic resonance spectroscopy. J Am Chem Soc 1975;97:4980–5.
[11] La Mar GN, Budd DL. Elucidation of the solution conformation of the A-ring in Vitamin D using proton coupling constants and a shift reagent. J Am Chem Soc 1974;96:7317–24.
[12] Kaneko C, Yamada S, Sugimoto A, Ishikawa M. Synthesis of 2β-hydroxycholecalciferol [2β-OH-D_3]. Chem Pharm Bull 1975;23:1616–9.

[13] Kaneko C, Yamada S, Sugimoto A, Ishikawa M. Synthesis and biological activity of 2α-hydroxyvitamin D_3. J Chem Soc Perkin I 1975:1104–7.
[14] Schonecker B, Prousa R, Reichenbacher M, Gliesing S, Kosan H, Droescher P, et al. Synthesis of 3β-acetoxy-1β,2β-epoxy-25-hydroxy-cholesta-5,7-diene and 2β,25-dihydroxyvitamin D_3. Bioorg Med Chem Lett 1993;3:1849–54.
[15] Silverstein RM, Bassler GC, Morrill TC, editors. Spectrometric identification of organic compounds. New York: John Wiley & Sons; 1991.
[16] Harvinga E. Vitamin D, example and challenge. Experientia 1973;29:1181–93.
[17] Rochel N, Wurtz JM, Mitschler A, Klaholz B, Moras D. The crystal structure of the nuclear receptor for Vitamin D bound to its natural ligand. Mol Cell 2000;5:173–9.
[18] Tocchini-Valentini G, Rochel N, Wurtz JM, Mitschler A, Moras D. Crystal structures of the Vitamin D receptor complexed to superagonist 20-epi ligands. Proc Natl Acad Sci USA 2001;98:5491–6.
[19] Vanhooke JL, Benning MM, Bauer CB, Pike JW, DeLuca HF. Molecular structure of the rat Vitamin D receptor ligand binding domain complexed with 2-carbon-substituted Vitamin D_3 hormone analogues and a LXXLL-containing coactivator peptide. Biochemistry 2004;43:4101–10.
[20] Tocchini-Valentini G, Rochel N, Wurtz JM, Moras D. Crystal structure of the Vitamin D nuclear receptor liganded with the Vitamin D side chain analogues calcipotriol and seocalcitol, receptor agonists of clinical importance. Insights into a structural basis for the switching of calcipotriol to a receptor antagonist by further side chain modification. J Med Chem 2004;47:1956–61.
[21] Shimizu M, Yamamoto K, Mihori M, Iwasaki Y, Morizono D, Yamada S. Two-dimensional alanine scanning mutational analysis of the interaction between the Vitamin D receptor and its ligands: studies of A-ring modified 19-norvitamin D analogs. J Steroid Biochem Mol Biology 2004;89/90: 75–81.
[22] Verboven C, Rabijns A, De Maeyer M, Van Baelen H, Bouillon R, De Ranter CD. A structure basis for the unique binding features of the human Vitamin D-binding protein. Nat Struct Biol 2002;9:131–6.
[23] Tsugawa N, Nakagawa K, Kurobe M, Ono Y, Kubodera N, Ozono K, et al. *In vitro* biological activities of a series of 2β-substituted analogues of 1α,25-dihydroxyvitamin D_3. Biol Pharm Bull 2000;23:66–71.